

Use of Artificial Intelligence to Reduce Radiation Exposure at Fluoroscopy-Guided Endoscopic Procedures

Ji Young Bang, MD, MPH¹, Matthew Hough, MS², Robert H. Hawes, MD¹ and Shyam Varadarajulu, MD¹

OBJECTIVES: Exposure to ionizing radiation remains a hazard for patients and healthcare providers. We evaluated the utility of an artificial intelligence (AI)-enabled fluoroscopy system to minimize radiation exposure during image-guided endoscopic procedures.

METHODS: We conducted a prospective study of 100 consecutive patients who underwent fluoroscopy-guided endoscopic procedures. Patients underwent interventions using either conventional or AI-equipped fluoroscopy system that uses ultrafast collimation to limit radiation exposure to the region of interest. The main outcome measure was to compare radiation exposure with patients, which was measured by dose area product. Secondary outcome was radiation scatter to endoscopy personnel measured using dosimeter.

RESULTS: Of 100 patients who underwent procedures using traditional (n = 50) or AI-enabled (n = 50) fluoroscopy systems, there was no significant difference in demographics, body mass index, procedural type, and procedural or fluoroscopy time between the conventional and the AI-enabled fluoroscopy systems. Radiation exposure to patients was lower (median dose area product 2,178 vs 5,708 mGy², P = 0.001) and scatter effect to endoscopy personnel was less (total deep dose equivalent 0.28 vs 0.69 mSv; difference of 59.4%) for AI-enabled fluoroscopy as compared to conventional system. On multivariate linear regression analysis, after adjusting for patient characteristics, procedural/fluoroscopy duration, and type of fluoroscopy system, only AI-equipped fluoroscopy system (coefficient 3,331.9 [95% confidence interval: 1,926.8–4,737.1, P < 0.001) and fluoroscopy duration (coefficient 813.2 [95% confidence interval: 640.5–985.9], P < 0.001) were associated with radiation exposure.

DISCUSSION: The AI-enabled fluoroscopy system significantly reduces radiation exposure to patients and scatter effect to endoscopy personnel (see Graphical abstract, Supplementary Digital Content, <http://links.lww.com/AJG/B461>).

SUPPLEMENTARY MATERIAL accompanies this paper at <http://links.lww.com/AJG/B440>, <http://links.lww.com/AJG/B441>, <http://links.lww.com/AJG/B461>

Am J Gastroenterol 2020;00:1–7. <https://doi.org/10.14309/ajg.0000000000000565>

BACKGROUND

Fluoroscopy is an integral part of both basic and advanced gastrointestinal endoscopy procedures such as stricture dilation, enteral feeding tube placement, double-balloon enteroscopy, endoscopic retrograde cholangiopancreatography (ERCP), and interventional endoscopic ultrasound (EUS). The use of fluoroscopy exposes patients, gastroenterologists, and endoscopy support personnel to ionizing radiation. Although exposure to high-dose-rate ionizing radiation has been shown to be associated with genomic instability (1,2), data indicate that exposure to even low-dose radiation, typically used for diagnostic imaging, may be associated with an increase in cancer mortality (3). The lifetime cancer risk is based on the effective dose (ED) of radiation received, which is measured in sieverts. Although the typical ED of

radiation for an abdominal computed tomography scan is approximately 10 mSv, with an associated lifetime risk of fatal cancer of approximately 1 in 2000 (4), the corresponding ED for an abdominal x-ray, barium enema, diagnostic, and therapeutic ERCP are 0.5, 5, 3.1, and 12.4 mSv, with estimated lifetime cancer risk of approximately 1 in 29,000, 1 in 3,000, 1 in 6,700, and 1 in 1,700, respectively (5,6). Although causal relationship is unclear, reports of fetal loss and neonatal death have been reported after ERCP in pregnant patients (7).

Radiation effects on tissues can be classified as deterministic and stochastic effects. Deterministic effects include cataract formation, infertility, skin injury, and hair loss. These reactions have been documented in patients receiving high radiation exposures while undergoing interventional cardiology and radiology procedures

¹Center for Interventional Endoscopy, AdventHealth, Orlando, Florida, USA; ²Department of Radiation Safety & Medical Physics, AdventHealth, Orlando, Florida, USA.
Correspondence: Shyam Varadarajulu, MD. E-mail: svaradarajulu@yahoo.com.

Received August 20, 2019; accepted February 3, 2020; published online March 18, 2020

and in interventional radiologists and cardiologists (8). Stochastic effects are more delayed and include radiation-induced cancers and genetic defects (9). Given the long lag time, these risks are inherently more difficult to estimate than tissue reactions. In a recent study conducted at a high-volume endoscopy center, the estimated dose equivalent at eye level was estimated to be 126 mSv for an endoscopist performing 500 therapeutic ERCPs per year (10). Consequently, exposure to ionizing radiation is considered a health hazard to patients and gastroenterologists and endoscopy support personnel. As such, appropriate measures to keep radiation exposure as low as reasonably achievable should be implemented. Professional societies such as the American Society for Gastrointestinal Endoscopy and the European Society of Gastrointestinal Endoscopy have published guidelines on radiation safety (11,12).

The 2 main sources of radiation during ERCP are the incident beam, which is the main source of radiation to the patient, and scatter radiation that emanates from the patient's body, which is the main source of radiation to individuals around the patient. Larger the radiation dose to the patient, the greater the scatter. Attempts to minimize radiation exposure include decreasing fluoroscopy time, using pulsed fluoroscopy, increasing the distance from radiation source, shielding, limiting magnification, using collimation, altering x-ray beam angulation, and avoiding use of C-arm units or over-couch x-ray systems (13–17). Use of personal protective equipment also reduces occupational exposure; however, many gastroenterologists performing ERCP do not routinely wear optimal protective (0.35 mm lead equivalent aprons, thyroid shield, lead glasses) clothing (14). In a survey of gastroenterologists, it was observed that only 52% of respondents reported wearing thyroid shield during fluoroscopy procedures (18). Moreover, even if worn, the protective wear fails to shield many parts of the body from radiation, including the brain and hands. Additionally, there is wide variation in fluoroscopy time and radiation exposure based on the level of endoscopist experience and the complexity of interventions undertaken (19–21). Finally, tracking fluoroscopy time requires conscious perception of being exposed to radiation, which can be difficult in the midst of a complex or challenging endoscopic intervention (22).

Given the risks of radiation exposure and inherent limitations of the preventive measures outlined, there is a need for an alternate technology that is seamless, intuitive, effective and preferably integrated within the fluoroscopy system itself. Such a technology would recognize key markers (site of intervention) within a given field (fluoroscopy image) and selectively deliver radiation to this region of interest (ROI) with minimal manual input. We hypothesized that this objective could be achieved by integrating artificial intelligence (AI) into the fluoroscopy (AIF) system whereby a trained deep neural network can recognize key markers and facilitate the selective delivery of radiation to a ROI.

The objective of the present study was to compare radiation exposure and scatter effect between AIF and conventional systems in patients undergoing fluoroscopy-guided endoscopic procedures.

METHODS

Study design

This prospective study was undertaken at the AdventHealth Center for Interventional Endoscopy in Orlando, Florida. Consecutive patients who required image guidance underwent endoscopic procedures using one of the 2 fluoroscopy systems, one integrated with AI that uses ultrafast collimation to limit radiation exposure (FluoroShield; Omega Medical Imaging, Sanford,

Florida) and the other using conventional technology (E-View; Omega Medical Imaging), with alternate patients assigned to each system type. Procedural indications were ERCP, EUS-guided drainage or radiopaque marker placement, and jejunal feeding tube or luminal stent placement. Pregnant patients and children were excluded. All authors had access to the study data and have reviewed and approved the final manuscript.

Study oversight

The study was approved by the AdventHealth institutional review board. Although patients provided informed consent for undergoing endoscopic procedures, given that the investigation involved minimal risk to patients without deviation from current standard of care, the board waived the requirements for providing study-related consent. The study was investigator-initiated and received no external funding.

Fluoroscopy systems

Conventional E-view. The system includes a 10-way motorized table for different patient angulations, 360° lead shielding protection on the image detector above the patient and all 3 sides of the table to reduce scatter radiation, a wide table top that can accommodate between 500 and 800 lbs of patient weight, 30 × 30 cm flat panel detector for visibility of a large anatomical area, 2 magnification modes for zooming and pulsed frequency to reduce the dose of ionizing radiation to the patient

AIF. The AIF platform is a technologically modified version of the E-view system with the objective of minimizing radiation exposure and is currently not available on fluoroscopy systems by other manufacturers. During an endoscopic procedure requiring fluoroscopy, the endoscopist is usually focused only on a small region of the displayed field of view. This small ROI typically correlates with procedural activity such as the movement of a guidewire or a catheter, deployment of endoprosthesis, injection of contrast, or placement of a marker. The larger area around the ROI, in the endoscopist's peripheral view, receives much less attention but is however needed for reference and orientation purposes. With the present technology, the larger area outside the ROI is exposed to the same radiation dosage as the small ROI.

The AIF system minimizes radiation exposure via a secondary collimator by constantly adjusting the shutter's lead blade orientation to block radiation to the area outside of the ROI for a majority of image frames and overlying the real-time ROI images over a full field of view image acquired a few frames before (Figure 1a–c). Image outside of the ROI aids only in the orientation, and this effect is not perceptible to the operator. The secondary collimator reduces radiation exposure to the patient by further reducing radiation that passes through the aperture of the primary collimator. The secondary collimator shutter's blades are controlled by an auto ROI processor that includes AI technology, ROI electronics unit, and/or the physician *via* an ROI control panel (see Figures 1 and 2, Supplementary Digital Content 1, <http://links.lww.com/AJG/B440>, <http://links.lww.com/AJG/B441>). Although the ROI is automatically targeted using AI, there is also an optional provision for manual control by the operator. **Training phase of convolutional neural network-based auxiliary reading model.** A critical element of the auto ROI processor is the key marker detection component which identifies the ROI. To this end, we used a convolutional neural network (CNN)-based algorithm, a type of artificial neural network used in deep learning and a method for analysis of visual imagery, to recognize ROI (key components) within a fluoroscopy image. The images

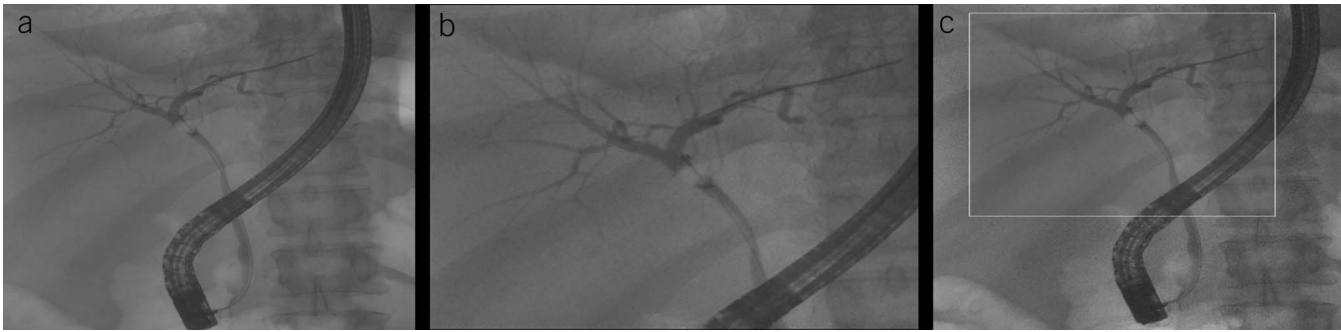


Figure 1. (a) Left image: Depiction of current standard with complete field of view (FOV) on x-ray. (b) Center image: Using artificial intelligence-enabled fluoroscopy technology, to minimize radiation exposure, the gastrointestinal endoscopist could collimate down to just the site of intervention. However, the complete FOV is reduced and contextual image information is lost in the periphery and therefore is impractical for clinical application. (c) Right image: The optimal approach whereby artificial intelligence processes the image data in real-time and controls an ultrafast collimator such that radiation exposure is minimized to the region of interest, such as an area of instrumentation. In high-reduction mode, artificial intelligence-enabled fluoroscopy captures a complete FOV image by opening the collimator at a 1,000 mS interval and then reregisters the full FOV background image with the collimated image and presents the seamlessly combined images, as shown here.

Video 1. A video showing the use of artificial intelligence-enabled fluoroscopy system in endoscopic retrograde cholangiopancreatography. The box outlined in white line refers to the region of interest, which in this case is balloon extraction of bile duct stones, to which radiation exposure is confined. The area surrounding the white box does not receive any radiation; however, the secondary collimator aperture is fully opened once per second to allow the background image data to refresh. (Watch the video at <http://links.lww.com/AJG/B442>.)

that were used in training and validation of the neural network were obtained from fluoroscopy-guided procedures performed at our endoscopy unit from August to November 2017. The images were split into a training dataset comprising 9,201 images and a testing dataset comprising 1,277 images. The images were annotated by trained personnel for key components such as catheters, guidewires, and endoscopes. These annotations were performed by drawing contours around the key markers and recording their coordinates. The training images and their corresponding annotations were then used to train the CNN (deep learning algorithm) (23), which took approximately 4 weeks in duration.

Validation of the CNN-based model. After training of the CNN model was completed, its performance was evaluated quantitatively on the testing image dataset. Evaluation was performed on each image by computing the Sørensen-Dice coefficient to measure the overlap between the automatic ROI and its corresponding manually annotated ROI (24). The average overlap over all the testing images was 95.3%. In addition, the performance of the complete auto ROI processor, integrated with the trained model, was evaluated qualitatively by a team of 3 trained personnel on 120 Video image sequences that were excluded from the training and testing datasets.

After completion of the validation phase, the trained model was integrated into the auto ROI processor of the fluoroscopy unit for clinical application. Once trained, tested, and validated, the system does not require further training for installation and use, and the algorithms, models, and their parameters do not change, adapt, or learn during the clinical application of a system. Although fully automated, the endoscopist can, at any time, manually adjust the ROI and/or turn it off entirely. The technology also provides options for high-reduction mode (secondary

collimator shutter is fully opened once per second to allow background image data to refresh), low reduction mode (secondary collimation shutter is fully opened twice per second), or no reduction (secondary collimator is disabled).

Radiation monitoring

Both fluoroscopy systems were operated by 3 certified radiology technicians (mean experience of 5 years) with the AIF system in high-reduction mode, and pulsed fluoroscopy was used in all patients at a frame rate of 12.5 frames/s. Radiation exposure to patients was measured using a dose area product (DAP) meter (VacuDAP Fluoro; VacuTec Meßtechnik GmbH, Dresden, Germany), which was integrated into both fluoroscopy systems. DAP is a measure of radiation dose delivered across the entire exposed field and is derived from the absorbed dose multiplied by the area irradiated (mGy cm^2). For each procedure, the following parameters were recorded: the fluoroscopy and procedural duration (min) and the DAP readings. Radiation scatter was measured using a thermoluminescence dosimeter (Luxel[®]; Landauer, Glenwood, IL) that was positioned identically on a stationary beam in both systems, precisely at a height of 4 feet (hip level) and 2 feet away from the fluoroscopy table. To obtain accurate readings, no other fluoroscopy-based procedures other than those related to the study were performed in either endoscopy suite. The dosimeter readings were summarized at the completion of 50 endoscopic procedures using each of the fluoroscopy systems.

Outcome measures

The primary outcome measure was to compare the radiation exposure in patients undergoing fluoroscopy-guided endoscopic procedures using AIF with conventional fluoroscopy systems. The secondary outcome measure was to compare the radiation scatter between the 2 fluoroscopy systems.

Sample size calculation

A 2-sided sample size calculation was performed based on the primary outcome measure of radiation exposure (DAP) to patients during fluoroscopy-guided endoscopic procedures. Assuming mean AIF to conventional fluoroscopy ratio of 0.6 and coefficient of variation of 1.0 based on the pilot system evaluation

Table 1. Patient characteristics

	Conventional system (n = 50)	AIF system (n = 50)	P value
Age (yr)			
Mean (SD)	58.2 (17.5)	63.9 (16.8)	
Median	58	66	0.070
IQR	44–72	52–79	
Range	7–90	27–92	
Gender, n (%)			
Female	28 (56.0)	27 (54.0)	0.841
Male	22 (44.0)	23 (46.0)	
Race, n (%)			
Asian	1 (2.0)	3 (6.0)	0.674
Black	8 (16.0)	5 (10.0)	
Hispanic	5 (10.0)	6 (12.0)	
White	36 (72.0)	36 (72.0)	
Body mass index (kg/m ²)			
Mean (SD)	28.6 (8.1)	26.3 (5.8)	
Median	27.3	26.1	0.152
IQR	24.5–31.0	22.3–28.5	
Range	15.7–60.4	17.7–49.1	

AIF, artificial intelligence-enabled fluoroscopy; IQR, interquartile range.

data, a sample size of 98 patients were estimated (49 patients per cohort) at 85% power and $\alpha = 0.05$. Sample size calculation was performed using PASS 15 Power Analysis and Sample Size Software (NCSS; LLC., Kaysville, UT) (25).

Statistical analysis

Continuous data were summarized as means with SD and medians with interquartile range (IQR) and range were compared using the Wilcoxon rank-sum test. Categorical data were summarized as frequencies with percentages and were compared using the χ^2 or Fisher exact test (as indicated).

Multiple linear regression and reverse stepwise multivariate linear regression analyses were performed to identify the factors associated with patient radiation exposure. The outcome variable was DAP, and clinically relevant variables such as the type of fluoroscopy system used, patient demographics, and procedure details were included as predictor variables. Two-sided *P*-values were reported for comparison of all outcome measures. Statistical significance was determined at *P* < 0.05. All statistical analyses were performed using Stata 14 (StataCorp LP, College Station, TX).

RESULTS

Patient characteristics and procedure details

Of the 100 consecutive patients who underwent fluoroscopy-guided endoscopic procedures from May 22 to June 30, 2019, alternate subjects were treated using the AIF system (n = 50) or the conventional fluoroscopy system (n = 50). There was no significant difference in patient demographics or body mass index between the groups (Table 1). There was also no significant difference in the types of interventions performed (>85% ERCP in

both cohorts), overall procedural or fluoroscopy duration, cumulative Air Kerma, and the number of spot images obtained between the groups (Table 2). With the exception of 2 subjects, the ROI was correctly identified by the autoprocessor in 48 patients (Figure 1a); manual control by the technician was required in these 2 patients to focus exposure to the ROI (esophageal stent placement in one and duodenal stent placement in one patient), and no clear reason was identified to account for the failure to identify the ROI. No difference in fluoroscopic image quality was observed between the 2 systems, and there were no adverse events related to either fluoroscopy system.

Outcomes

Radiation exposure to patients was significantly lower for the AIF system as compared to the conventional fluoroscopy system, with DAP of 2,178 mGy m² (IQR 1,308.6–4,317.7) vs 5,708 mGy m² (IQR 1,965.7–7,953.3), *P* = 0.001, respectively (Table 2). The radiation scatter was 59.4% less for the AIF system as compared to the conventional fluoroscopy system, with deep dose equivalent dosimeter measurement of 0.28 vs 0.69 mSv. On multivariate linear regression analysis, after adjusting for patient characteristics, procedural/fluoroscopy duration, number of spot images taken, and type of fluoroscopy system, only the AIF system (coefficient 3,331.9 [95% confidence interval: 1,926.8–4,737.1, *P* < 0.001) and fluoroscopy duration (coefficient 813.2 [95% confidence interval: 640.5–985.9], *P* < 0.001) were associated with radiation exposure (Table 3).

DISCUSSION

The present study demonstrates that an AI-enabled system correctly identifies the region of interest in a fluoroscopy field,

Table 2. Procedure details and radiation exposure readings

	Conventional system (n = 50)	AIF system (n = 50)	P value
Type of procedure, n (%)			
ERCP biliary	40 (80.0)	40 (80.0)	0.407
ERCP pancreatic	6 (12.0)	4 (8.0)	
EUS-guided interventions	1 (2.0)	2 (4.0)	
Luminal stent placement	1 (2.0)	4 (8.0)	
Other	2 (4.0)	0	
Total procedure duration (min)			
Mean (SD)	28.0 (14.4)	27.7 (19.5)	
Median	28.5	20.5	0.515
IQR	15–35	14–38	
Range	4–68	2–78	
Total no. of fluoroscopic images taken			
Mean (SD)	8.4 (5.2)	9.1 (4.0)	
Median	7	9	0.155
IQR	5–10	6–12	
Range	1–30	1–18	
Total fluoroscopy duration (min)			
Mean (SD)	4.4 (3.0)	5.2 (4.9)	
Median	3.3	3.8	0.707
IQR	1.7–6.2	2.1–6.1	
Range	1.1–12.3	1.1–22.4	
Radiation exposure to patients—Dose area product (mGy cm ²)			
Mean (SD)	6,427 (5,167)	3,777 (4,465)	
Median	5,708	2,178	0.001
IQR	1,966–7,953	1,309–4,318	
Range	473–22,017	92–24,969	
Cumulative Air Kerma (mGy) ^a			
Mean (SD)	155 (149)	147 (137)	
Median	124	107	0.793
IQR	51–173	63–188	
Range	14–782	3–579	
Scatter effect—total dosimeter measurement ^b (mSv)			
Deep dose equivalent	0.69	0.28	—
Lens dose equivalent	0.69	0.28	—
Shallow dose equivalent	0.68	0.26	—

AIF, artificial intelligence-enabled fluoroscopy; DAP, dose area product; ERCP, endoscopic retrograde cholangiopancreatography; EUS, endoscopic ultrasound; IQR, interquartile range.

^aAir Kerma is the energy released in a unit mass of air and measures radiation dose at a particular spot but not the overall dose to the patient (which is measured by DAP).

^bDeep dose equivalent = external whole-body exposure; Lens dose equivalent = external exposure of the lens; Shallow dose equivalent = external exposure of the skin or extremity.

and when compared with conventional technology, it significantly reduces radiation exposure and scatter effect. Although the utility of AI in other areas of digestive diseases, such as discerning pathological lesions from normal variants on

capsule endoscopy images, has been proven (26), to our knowledge, this is the first investigation to demonstrate its capability to execute a purposeful reactive action based on image interpretation.

Table 3. Multiple linear regression analysis and reverse stepwise multivariate linear regression analysis to identify factors associated with dose area product

Variable	Regression coefficient	95% CI	P value
Multiple linear regression analysis			
Age (yr)	4.1	−39.1 to 47.3	0.851
Body mass index (kg/m ²)	75.2	−28.0 to 178.4	0.151
Total procedure duration (min)	1.95	−51.6 to 55.5	0.942
Total fluoroscopy duration (min)	777.6	552.3 to 1,002.9	<0.001
Total no. of fluoroscopic images taken	75.1	−85.9 to 236.1	0.357
Fluoroscopy system type: conventional vs AIF	3,210.5	1,754.5 to 4,666.5	<0.001
Reverse stepwise multivariate linear regression analysis			
Total fluoroscopy duration (min)	813.2	640.5 to 985.9	<0.001
Fluoroscopy system type: conventional vs AIF	3,331.9	1,926.8 to 4,737.1	<0.001

AIF, artificial intelligence-enabled fluoroscopy; CI, confidence interval.

Despite several reports on the hazards of radiation exposure and scatter (27,28), barriers to achieving optimal radiation protection persist. Although it has been shown that a 20-minute educational program on the ideal use of fluoroscopic machine settings results in significant reduction in radiation exposure, in a recent survey of 159 endoscopists, predominantly from academic medical centers, 57% reported receiving no training on the operation of fluoroscopy systems despite more than 60% using personally controlled fluoroscopy systems themselves during procedures (29,30). Although low-resolution imaging is associated with less radiation, complex maneuvers in the pancreaticobiliary system mandate high resolution for optimal visualization (20). Other attempts to minimize radiation exposure have included erecting a mobile shield barrier, using EUS guidance in lieu of fluoroscopy, performing 2-stage procedures in pregnant patients, and installing flashing warning lights to reduce fluoroscopy time (22,31–33). However, none of these attempts are ideal because they require frequent manual input and oftentimes involve multiple operators with varying levels of procedural experience and radiation protection awareness. Nevertheless, these barriers can be overcome if the fluoroscopy system possesses the inherent ability to autoregulate radiation exposure.

In the present study, the dosimeter recorded scatter radiation of only 0.28 mSv for 50 procedures with AIF, which when extrapolated is less than 3 mSv for 500 procedures, a level that is significantly less than the recommended annual limit of 20 mSv (34). Although scatter radiation was 60% greater with conventional fluoroscopy as compared to AIF, it was still less than radiation exposure reported with use of C-arm technology (10). In a previous study, we have shown that scatter radiation exposure was 6-fold less even with use of conventional fluoroscopy described in this study as compared to standard C-arm technology (35), an observation confirmed by others (10). Both fluoroscopy systems used in the present study were state of the art with lead shielding that significantly reduces radiation scatter. Although high-quality data on the risk of cancer from occupational exposure to ionizing radiation are lacking, given the assumed linear increase in risk, even with low-

dose radiation (3), it is important to limit radiation exposure to the lowest level possible, but without compromising the outcome of endoscopic interventions. This is particularly relevant in some unique circumstances—patients and endoscopy personnel who are pregnant or of child bearing age, children, endoscopists performing high-volume fluoroscopy-guided procedures, and endoscopy personnel designated to working in fluoroscopy suites. We also believe that these observations are pertinent to other specialties of medicine such as interventional cardiology and radiology, where a large volume of procedures are performed under fluoroscopic guidance.

A limitation of the current system is that learning algorithms powering technical systems require training on large labeled datasets. However, supplying training data for all situations may not always be possible. In the present study, in 2 of the 50 procedures using AIF, manual control was required to target the ROI. In the future, programs based on reinforcement learning, a technique where a computer learns how to behave in a given situation without any instructions, may target the ROI more precisely and consistently. The findings of our single center study are preliminary and require validation by other investigators. Because the AIF mode was evident by the presence of a box around the ROI, it was not possible to perform a blinded assessment of the image quality between systems. In our experience, the fluoroscopic image quality was equivalent and there was no need to switch off the AI mode in any of the 50 patients who underwent procedures using this novel technology. Finally, when deciding on the implementation of new technology, it is important to consider not only the efficacy and safety but also cost. Although decisions regarding the monetary value of the demonstrated reduction in radiation exposure will be necessary to determine whether healthcare institutions will choose to adopt this technology, given the obvious advantages demonstrated in this study, the manufacturer has integrated AI in all fluoroscopy systems currently being produced.

In summary, the development of an AI-enabled fluoroscopy system is an important advancement in the field of gastrointestinal

endoscopy because it significantly reduces radiation exposure to patients and scatter effect to endoscopy personnel.

CONFLICTS OF INTEREST

Guarantor of the article: Shyam Varadarajulu, MD.

Specific author contributions: J.Y.B.: study design, endoscopist performing procedures in the trial, acquisition of data, analysis and interpretation of data, statistical analysis, drafting the manuscript, and critical revision of the manuscript. S.V.: study concept and design, endoscopist performing procedures in the trial, interpretation of the data, drafting the manuscript, and critical revision of the manuscript. R.H.: endoscopist performing procedures in the trial and critical revision of the manuscript. M.H.: critical revision of manuscript.

Financial support: None to report.

Potential competing interests: J.Y.B.: consultant for Olympus America Inc. and Boston Scientific Corporation. S.V.: consultant for Boston Scientific Corp., Olympus America Inc., Covidien, and Creo Medical. R.H.: consultant for Boston Scientific Corp., Olympus America Inc., Covidien, Creo Medical, NinePoint Medical, and Cook Medical. M.H.: No conflicts of interest.

ClinicalTrials.gov identifier: NCT03985488.

Study Highlights

WHAT IS KNOWN

- ✓ The use of fluoroscopy exposes patients and medical personnel to the effects of ionizing radiation.

WHAT IS NEW HERE

- ✓ An AIF system minimizes radiation exposure via a secondary collimator by blocking radiation to the area outside the region of interest.
- ✓ The AIF system significantly reduces radiation exposure to patients and scatter effect to endoscopy personnel by 60%.

REFERENCES

1. Bouffler S, Silver A, Cox R. Mechanistic and genetic studies of radiation tumorigenesis in the mouse—implications for low dose risk estimation. *J Radiol Prot* 2002;22:A11–6.
2. Jaffe D, Bowden GT. Ionizing radiation as an initiator: Effects of proliferation and promotion time on tumor incidence in mice. *Cancer Res* 1987;47:6692–6.
3. Richardson DB, Cardis E, Daniels RD, et al. Risk of cancer from occupational exposure to ionising radiation: Retrospective cohort study of workers in France, the United Kingdom, and the United States (INWORKS). *BMJ* 2015;351:h5359.
4. Brenner DJ, Hall EJ. Computed tomography—an increasing source of radiation exposure. *N Engl J Med* 2007;357:2277–84.
5. Larkin CJ, Workman A, Wright RE, et al. Radiation doses to patients during ERCP. *Gastrointest Endosc* 2001;53:161–4.
6. Linet MS, Slovis TL, Miller DL, et al. Cancer risks associated with external radiation from diagnostic imaging procedures. *CA Cancer J Clin* 2012;62:75–100.
7. Jamidar PA, Beck GJ, Hoffman BJ, et al. Endoscopic retrograde cholangiopancreatography in pregnancy. *Am J Gastroenterol* 1995;90:1263–7.
8. Rehani MM, Vano E, Ciraj-Bjelac O, et al. Radiation and cataract. *Radiat Prot Dosimetry* 2011;147:300–4.
9. Kleinerman RA. Cancer risks following diagnostic and therapeutic radiation exposure in children. *Pediatr Radiol* 2006;36:121–5.
10. Muniraj T, Aslanian HR, Laine L, et al. A double-blind, randomized, sham-controlled trial of the effect of a radiation-attenuating drape on radiation exposure to endoscopy staff during ERCP. *Am J Gastroenterol* 2015;110:690–6.
11. ASGE Technology Committee; Pedrosa MC, Pedrosa MC, Farraye FA, et al. Minimizing occupational hazards in endoscopy: Personal protective equipment, radiation safety, and ergonomics. *Gastrointest Endosc* 2010;72:227–35.
12. Dumonceau JM, Garcia-Fernandez FJ, Verdun FR, et al. Radiation protection in digestive endoscopy: European Society of Digestive Endoscopy (ESGE) guideline. *Endoscopy* 2012;44:408–21.
13. Campbell N, Sparrow K, Fortier M, et al. Practical radiation safety and protection for the endoscopist during ERCP. *Gastrointest Endosc* 2002;55:552–7.
14. Ho IK, Cash BD, Cohen H et al. Radiation exposure in gastroenterology: Improving patient and staff protection. *Am J Gastroenterol* 2014;109:1180–94.
15. Uradomo LT, Goldberg EM, Darwin PE. Time-limited fluoroscopy to reduce radiation exposure during ERCP: A prospective randomized trial. *Gastrointest Endosc* 2007;66:84–9.
16. Kurihara T, Itoi T, Sofuni A, et al. Novel protective lead shield and pulse fluoroscopy can reduce radiation exposure during the ERCP procedure. *Hepatogastroenterology* 2012;59:709–12.
17. Johlin FC, Pelsang RE, Greenleaf M. Phantom study to determine radiation exposure to medical personnel involved in ERCP fluoroscopy and its reduction through equipment and behavior modifications. *Am J Gastroenterol* 2002;97:893–7.
18. Campbell N, John V, Sparrow K et al. Radiation safety and protection among ERCP endoscopists. *Can J Gastroenterol* 2000;14:48A.
19. Jorgensen JE, Rubenstein JH, Goodsitt MM, et al. Radiation doses to ERCP patients are significantly lower with experienced endoscopists. *Gastrointest Endosc* 2010;72:58–65.
20. Syed AR, Garg MS, Patel P, et al. Fluoroscopy dose and time characteristics during endoscopic retrograde cholangiopancreatography (ERCP). *Surg Laparosc Endosc Percutan Tech* 2019;29:22–5.
21. Hayashi S, Nshida T, Matsubara T, et al. Radiation exposure dose and influencing factors during endoscopic retrograde cholangiopancreatography. *PLoS One* 2018;13(12):e0209877.
22. Zeng HZ, Liu Q, Chen HL, et al. A pilot single-center prospective randomized trial to assess the short-term effect of a flashing warning light on reducing fluoroscopy time and radiation exposure during ERCP. *Gastrointest Endosc* 2018;88:261–6.
23. Goodfellow I, Bengio Y, Courville A. *Deep Learning*, 1 edn. The MIT Press: Cambridge, MA, 2016, chapter 9, pp 321–59.
24. Zijdenbos AP, Dawant BM, Margolin RA, et al. Morphometric analysis of white matter lesions in MR images: Method and validation. *IEEE Trans Med Imaging* 1994;13:716–24.
25. Chow SC, Shao J, Wang H, et al. *Sample Size Calculations in Clinical Research*. Chapman and Hall: New York, NY, 2017.
26. Ding Z, Shi H, Zhang H, et al. Gastroenterologist-level identification of small bowel diseases and normal variants by capsule endoscopy using a deep-learning model. *Gastroenterology* 2019;157:1044–54.e5.
27. Menon S, Mathew R, Kumar M. Ocular radiation exposure during endoscopic retrograde cholangiopancreatography: A meta-analysis of studies. *Eur J Gastroenterol Hepatol* 2019;31:463–70.
28. Zagorska A, Romanova K, Hristova-Popova J, et al. Eye lens exposure to medical staff during endoscopic retrograde cholangiopancreatography. *Phys Med* 2015;31:781–4.
29. Barakat MT, Thosani NC, Huang RJ, et al. Effects of a brief educational program on optimization of fluoroscopy to minimize radiation exposure during endoscopic retrograde cholangiopancreatography. *Clin Gastroenterol Hepatol* 2018;16:550–7.
30. Sethi S, Barakat MT, Friedland S, et al. Radiation training, radiation protection, and fluoroscopy utilization practices among US therapeutic endoscopists. *Dig Dis Sci* 2019;64:2455–66.
31. Chung KH, Park YS, Ahn SB, et al. Radiation protection effect of mobile shield barrier for the medical personnel during endoscopic retrograde cholangiopancreatography: A quasi-experimental prospective study. *BMJ Open* 2019;20(9):e027729.
32. Jiang XW, Tang SH, Yang JQ, et al. Ultrasound-guided endoscopic biliary drainage: A useful drainage method for biliary decompression in patients with biliary obstructions. *Dig Dis Sci* 2014;59:161–7.
33. Sharma SS, Maharshi S. Two stage endoscopic approach for management of choledocholithiasis during pregnancy. *J Gastrointest Liver Dis* 2008;17:183–5.
34. Rehani MM, Ciraj-Bjelac O, Vano E, et al. ICRP Publication 117. Radiological protection in fluoroscopically guided procedures performed outside the imaging department. *Ann ICRP* 2010;40:1–102.
35. Bang JY, Hawers RH, Varadarajulu S. Do fluoroscopy systems influence the level of scatter radiation exposure during endoscopic procedures? *Dig Endosc* 2015;27:629.